

Multi-modal Fusion for Single-Stage Continuous Gesture Recognition

Harshala Gammulle, *Member, IEEE*, Simon Denman, *Member, IEEE*, Sridha Sridharan, *Life Senior Member, IEEE*, Clinton Fookes, *Senior Member, IEEE*.

Abstract—Gesture recognition is a much studied research area which has myriad real-world applications including robotics and human-machine interaction. Current gesture recognition methods have heavily focused on isolated gestures, and existing continuous gesture recognition methods are limited by a two-stage approach where independent models are required for detection and classification, with the performance of the latter being constrained by detection performance. In contrast, we introduce a single-stage continuous gesture recognition model, that can detect and classify multiple gestures in a single video via a single model. This approach learns the natural transitions between gestures and non-gestures without the need for a pre-processing segmentation stage to detect individual gestures. To enable this, we introduce a multi-modal fusion mechanism to support the integration of important information that flows from multi-modal inputs, and is scalable to any number of modes. Additionally, we propose Unimodal Feature Mapping (UFM) and Multi-modal Feature Mapping (MFM) models to map uni-modal features and the fused multi-modal features respectively. To further enhance the performance we propose a mid-point based loss function that encourages smooth alignment between the ground truth and the prediction. We demonstrate the utility of our proposed framework which can handle variable-length input videos, and outperforms the state-of-the-art on two challenging datasets, EgoGesture, and IPN hand. Furthermore, ablative experiments show the importance of different components of the proposed framework.

Index Terms—Gesture Recognition, Spatio-temporal Representation Learning, Temporal Convolution Networks.

I. INTRODUCTION

THE computer-aided recognition of gestures has a vast number of applications including human-computer interaction, robotics, sign language recognition, gaming and virtual reality control. Due to its diverse applications, gesture recognition has gained much attention in the computer vision domain.

Most gesture recognition approaches are based on recognising isolated gestures [1]–[3] where an input video is manually segmented into clips that each contain a single isolated gesture. In a real-world scenario where gestures are performed continuously, methods based on isolated gestures are not directly applicable, and thus do not translate to a natural setting. As such, recent approaches [4]–[6] aim to recognise

gestures in the continuous original (i.e. unsegmented) video where multiple gesture categories, including both gestures and non-gesture actions, are included. These continuous gesture recognition approaches are formulated in two ways: two-stage [5]–[7] and single-stage [8] methods. The two-stage approach is built around using two models: one model to perform gesture detection (also known as gesture spotting), and another for gesture classification. In [6] the authors proposed a two-stage method where gestures are first detected by a shallow 3D-CNN and when a gesture is detected it activates a deep 3D-CNN classification model. Another work [5] proposed utilising a Bidirectional Long Short-Term Memory (Bi-LSTM) to detect gesture while the authors use a combination of two 3D Convolution Neural Networks (3D-CNN) and a Long Short-Term Memory (LSTM) network to process multi-modal inputs for gesture classification.

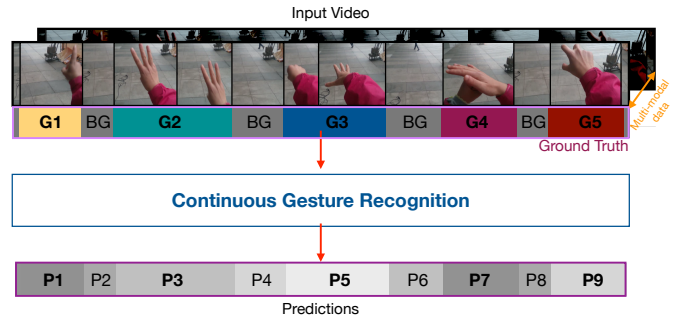


Fig. 1. Single-stage Continuous Gesture Recognition: The model is fed with a multi-modal (RGB, Depth etc.) feature sequence and the ground truth label sequence. The ground truth can belong to a particular gesture or a non-gesture (BG) class. During training, using the ground-truth the model learns to map from the input frames to the corresponding gesture class.

Single-stage approaches originate from the action recognition domain [9], [10], where frames that do not contain an action are labelled ‘background’ (similar to the non-gesture class). In contrast to two-stage methods, single-stage methods use only a single model which directly performs the gesture classification. Fig. 1 illustrates the typical structure of a single-stage approach where the recognition is performed by considering all the gesture classes together with the non-gesture class. In addition to being simpler than two-stage methods, single stage methods avoid the potential issue of errors being propagated between stages. For example, in a two-stage method, if the detector makes an error estimating the start or end of a gesture sequence this error is propagated through to the classification process. Hence, in two-stage

H. Gammulle, S. Denman, S. Sridharan and C. Fookes are with the Signal Processing, Artificial Intelligence and Vision Technologies (SAIVT) Lab, Queensland University of Technology, Brisbane, Australia.
E-mail: pranali.gammulle@qut.edu.au

methods, classifier performance is highly dependent on the robustness of the detector, further increasing the appeal of single-stage methods. However, we observe that two-stage methods are the popular choice among researchers when performing continuous gesture recognition. This is largely due to the challenges that a single network should address when performing both gesture localisation and recognition tasks, concurrently.

Several gesture recognition approaches have also exploited multi-modal data and have shown improved results through fusion [1], [5]. In [1], the authors introduce a simple neural network module to fuse features from two modes for the two-stage gesture recognition task. However, for continuous gesture recognition, any fusion scheme must consider that the input sequence includes multiple gestures that evolve temporally. Hence, using a simple attention layer to fuse domains restricts the learning capacity as the model attention is applied to the complete sequence, ignoring the fact that there are multiple gesture sub-sequences, and potentially leading to some individual gestures being suppressed.

In this paper we propose a novel single-stage method for continuous gesture recognition. By using a single-stage approach we expect the classification model to learn natural transitions between gestures and non-gestures. However, directly learning the gestures from a continuous unsegmented video is much more challenging as it requires the model to detect the transitions between gesture classes and recognise gestures/non-gestures simultaneously. To improve performance we consider multiple modalities and introduce a novel fusion module that extracts multiple feature sub-sequences from the multi-modal input streams, considering their temporal order. The proposed fusion module preserves this temporal order and enables the learning of discriminative feature vectors from the available modalities. To aid the model learning, we propose a novel mid-point based loss function, and perform additional experiments to prove the effectiveness of the proposed loss.

Figure 2 illustrates the architecture of our proposed framework. In the first stage of the model, semantic features from each mode are extracted via a feature extractor, and extracted features are passed through a Unimodal Feature Mapping (UFM) block. We maintain separate UFM blocks for each stream. The outputs of all UFM blocks are used by the proposed fusion modules which learns multi-modal spatio-temporal relationships to support the recognition process. The output of the fusion model is passed through the Multi-modal Feature Mapping (MFM) block which performs the final classification. The model is explicitly designed to handle variable length video sequences. Through evaluations on two continuous gesture datasets, EgoGesture [11] and IPN hands [4], we show that our proposed method achieves state-of-the-art results. We also perform extensive ablation evaluations, demonstrating the effectiveness of each component of the model. Furthermore, we illustrate the scalability of our proposed fusion model by performing continuous gesture recognition with two and three modes.

In summary our contributions are as follows,

- We propose a single-stage continuous gesture recognition

model, and utilises only a single model to achieve gesture detection and classification directly.

- We introduce a novel temporal multi-modal feature fusion mechanism, which preserves the temporal order of the inputs in the fusion process and supports the final classification task.
- We introduce a novel mid-point based loss function, which encourages smooth transitions between different gesture classes and enhances learning.
- We demonstrate our proposed framework is able to handle variable-length input videos, and significantly outperform the state-of-the-art results on two challenging data-sets.
- Through extensive ablation evaluations, we show the effectiveness of each of the proposed novelties in our framework.

II. RELATED WORKS

Gesture recognition has been an extensively studied area in computer vision as it facilitates multiple applications. Early approaches used handcrafted feature recognition systems [12]–[15]. For example, in [12] the authors proposed a spatio-temporal feature named Mixed Features around Sparse key-points (MFSK), which is extracted from RGB-D data. In [13] the authors propose to extract a visual representation for hand motions using motion divergence fields. Other methods are based on extracting Random Occupancy Pattern (ROP) features [16], Super Normal Vectors (SNV) [15], and improved dense trajectories [17]. However, these hand-crafted feature methods rely solely on human domain knowledge and risk failing to capture necessary information that may greatly contribute towards correct recognition.

Subsequently, attention has shifted to deep network-based approaches [18]–[22] due to their ability to learn task-specific features automatically, without being totally reliant on the domain knowledge of the researcher. As such, most recent gesture recognition methods use deep networks [1], [4], [6], [23]–[25] and have demonstrated superior results to their hand-crafted counterparts.

Deep learning methods have considered gesture recognition in two ways: isolated gesture recognition [1], [26], [27]; and continuous gesture recognition [6], [24]. Isolated gesture recognition uses segmented gesture videos containing a single gesture per video, and is a naive and simplified way of performing gesture recognition which does not reflect the overall real-world challenge gesture recognition poses. In [26], the authors proposed three variants of 3D CNNs which are able to learn spatio-temporal information through their hierarchical structure to learn to recognise isolated gestures. [1] proposed a fusion unit to integrate and learn information that flows through two uni-modal CNN models to support isolated gesture recognition. [28] introduced a multi-modal training/uni-modal testing approach where the authors embed the knowledge from individual 3D-CNN networks, forcing them to collaborate and learn a common semantic representation to recognise isolated gestures. However, the simplicity of isolated gesture recognition methods prevents their direct application for real-world tasks as the input video contains

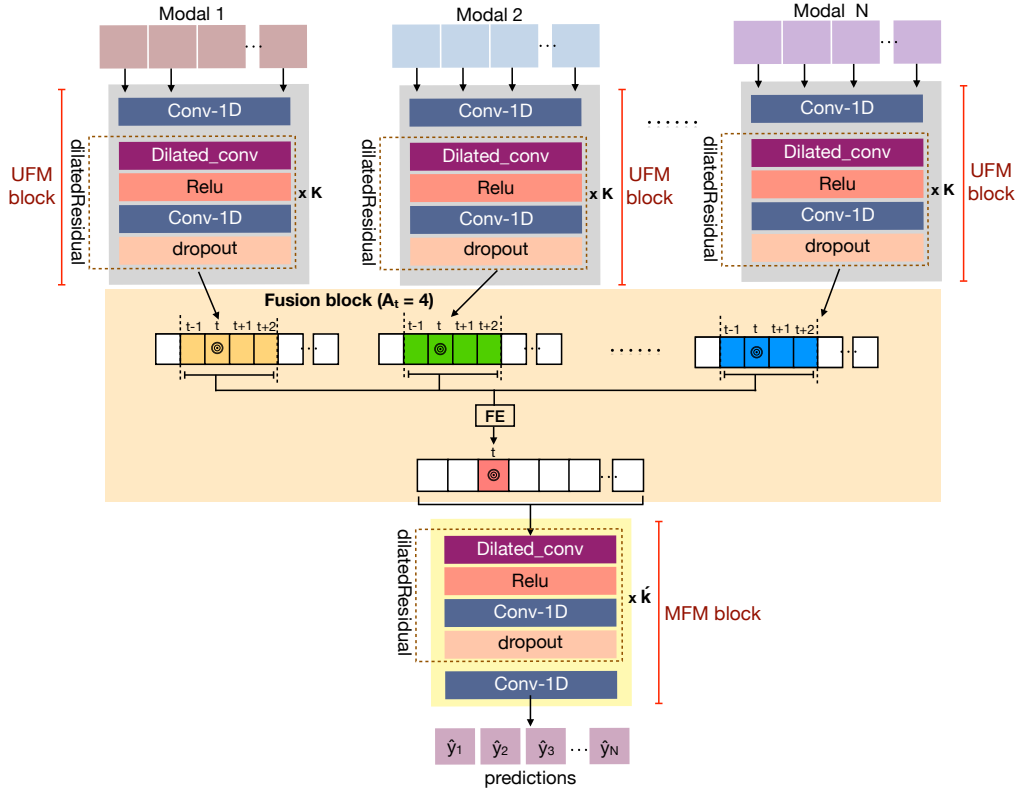


Fig. 2. Proposed single-stage framework: The data from each mode is passed through a pre-trained feature extractor and subsequently through separate Unimodal Feature Mapping (UFM) blocks. The output of each UFM block is fused by the proposed fusion block which learns discriminative features from each mode, considering the temporal order of the data. This aids the final gesture classification which is performed by the Multi-modal Feature Mapping (MFM) block.

multiple sequential gestures that must first be segmented. Hence focus has turned to developing methods for recognition of gestures in unsegmented (i.e. continuous) video streams [6].

In an unsegmented video, as there are sub-sequences containing both gestures and non-gestures, a typical model first detects gesture regions (also known as gesture spotting [11]) prior to recognising each of these gestures. [6] formulated a two-stage framework to carry out the detection and classification of continuous gestures, where their detection method first performs gesture detection and the classification model is activated only when a gesture is detected. However, these two-stage methods require two separate networks to perform gesture detection and classification respectively.

To the best of our knowledge [8], [11] are the only existing single-stage continuous gesture recognition methods. In [8] the authors employ an RNN to predict the gesture labels for input frame sequence. In [29] the authors utilise a C3D model to classify the continuous gestures. The model sequentially slides over the input video and outputs a single gesture class representing the gesture within that input window, including the non-gesture class. They propose to further improved the gesture prediction method by employing a Spatio-Temporal Transfer Module (STTM) [29] and an LSTM network where an LSTM predicts the gesture labels based on the C3D features. However, these methods fail to achieve comparative accuracies when evaluated against two-stage methods. We believe this is due to the simplistic nature of the architecture,

which could not handle the complexities within the single-stage framework.

Action and gesture recognition are related problem domains, where significant developments have occurred compared to gesture recognition domain. Similar to continuous gesture recognition, the task of continuous action recognition (also known as temporal action segmentation) has been investigated using various strategies [9], [10], [30], [31]. However, most temporal action segmentation methods are single-stage methods where detection and classification is performed by a single network. Single-stage methods offer advantages over two-stage methods in that there is only a single model and errors from the first stage (the detector) are not propagated to the second stage (the classifier). Furthermore, a single stage model can learn not only a single gesture sequence, but also leverage information on how different types of gestures are sequentially related. [9] introduced Temporal Convolution Networks (TCN) that utilise a hierarchy of temporal convolutions. In [10], the authors have extended the ideas of [9] and introduced a multi-stage model for action segmentation, where each stage is composed of a set of dilated temporal convolutions that generate predictions at each stage.

Motivated by previous action segmentation methods [9], [10], we propose a single-stage method for continuous gesture recognition. Although in [1], [28] multi-modal fusion or information sharing methods are proposed for gesture recognition, these fusion strategies have limited applicability to the single

stage paradigm. When sequences are segmented all frames are part of the same gesture, hence, a simple attention or concatenation of the features can produce good results as all the information relates to the one gesture. In contrast, in a single-stage model the input to the classifier contains multiple gesture sequences and non-gesture frames. Hence, the fusion strategy should understand how these sub-sequences are temporally related and filter out the most relevant information considering this temporal order. To this end, we introduce a fusion mechanism that preserves this temporal accordance and that can be applied to two or more modalities for continuous gesture recognition.

III. METHOD

We introduce a novel framework to support multi-modal single-stage video-based classification tasks such as gesture recognition. In the introduced framework, first the videos from each mode are passed through feature extractors, and the extracted deep features are subsequently passed through individual unimodal networks which we term Unimodal Feature Mapping (UFM) blocks. The output feature vector of each UFM block is used by the proposed fusion block and which learns a discriminative feature vector that is input to the Multi-modal Feature Mapping (MFM) block to perform classification. Figure 2 illustrates the overall model architecture.

Our framework can be used with segmented or unsegmented videos, that may be composed of one or more gesture classes, and supports the fusion of any number of modalities greater than 1. Each feature stream that belongs to a specific mode is required to pass through that mode's UFM block prior to fusion.

The task our approach seeks to solve can be defined as follows: given a sequence of video frames $X^i = \{x_1^i, x_2^i, \dots, x_T^i\}$, where $i = 1, 2, \dots, M$ (M number of modalities), we aim to infer the gesture class label for each time step t (i.e. $\hat{y}_1, \hat{y}_2, \dots, \hat{y}_T$).

In the following sections, we provide a detailed description of the models and the proposed loss formulation.

A. Unimodal Feature Mapping (UFM) Block

Video frames for a given modality are passed through a feature extractor (each mode has its own feature extractor to learn a mode specific representation), and the extracted features are the input to the UFM block. Through the UFM block, we capture salient features related to a specific modality and learn a feature vector suitable for feature fusion. As shown in Figure 2, this uni-modal network is composed of temporal convolution layers and multiple dilated residual blocks, where each dilated residual block is composed of a dilated convolution layer followed by a non-linear activation function and a 1×1 convolution-BatchNorm-ReLu [32] layer. We take inspiration from [10], where the authors utilize the residual connections to facilitate gradient flow. As in [10], [33], we use a dilation factor that is doubled at each layer and each layer is composed of an equal number of convolutional filters.

B. Fusion Block

The output vectors of the UFM blocks are passed through the fusion block, which extracts temporal features from the uni-modal sequences, considering their temporal accordance with the current time step. Feature fusion is performed using the attention level parameter. This parameter defines the feature units that should be selected from the output vector of each UFM block at a given time. An illustration is given in Figure 3.

1) *Attention Level parameter (A)*: Let $V_t^1, V_t^2, \dots, V_t^M$ be the output feature vectors from the UFM blocks representing the M modalities, where $t = 1, 2, \dots, T$. By considering the value set for the parameter A the algorithm decides which feature units from each vector should be selected for the fusion at time t . This selection criteria is defined based on the fact that multi-modal feature streams are synchronised and the features from the temporal neighbours at a particular timestamp should carry knowledge informative for the gesture class of that frame, while distant temporal neighbours do not carry helpful information (as they are likely from different gesture classes). Based on whether the A is even or odd, we calculate the position increment (i_{inc}) and decrement (i_{dec}) values as shown below. Here, i_{inc} defines the number of units ahead we should consider during the fusion, while i_{dec} defines the number of units behind that should be selected.

if A is even (i.e. $A \% 2 = 0$) **then**
 $i_{inc} = A/2$ and $i_{dec} = (A - 2)/2$
else if A_t is odd (i.e. $A \% 2 = 1$) **then**
 $i_{inc} = i_{dec} = (A - 1)/2$
end if

Once i_{inc} and i_{dec} are calculated, at t the units from $t - i_{dec}$ to $t + i_{inc}$ are selected from each feature vector. This sub feature vector is given by,

$$S_t^i = [V_{t-i_{dec}}^i, \dots, V_t^i, \dots, V_{t+i_{inc}}^i], \quad (1)$$

where $i = 1, 2, \dots, M$. As shown in Figure 4, when the attention level is 4, 4 feature units (from $t - 1$ to $t + 2$) are selected from each vector from the UFM.

2) *Feature Enhancer (FE)*: At each time step t , the feature enhancer receives computed sub-vectors S_t^i s from each UFM, where i indicates the modality, and concatenates these sub-vectors generating an augmented vector η_t ,

$$\eta_t = [S_t^1, \dots, S_t^i, \dots, S_t^M]. \quad (2)$$

If each feature unit is of dimension d and the attention level is A , then η_t will have shape, $(d, A \times M)$. We then utilise the proposed Feature Enhancer (FE) block, which is inspired by the squeeze and excitation block architecture introduced in [34], to allow the model to identify informative features from the fused multi-modal features, enhancing relevant feature units and suppressing uninformative features. However, the squeeze-and-excitation block of [34] considers the overall 2D/3D CNN layer output and enhances features considering their distribution across channels. In contrast, we propose to enhance features within sub-feature vectors, V^i s, for each t . Through the FE block, features from each sub-feature vector are enhanced by explicitly modelling the inter-dependencies

between channels, further supporting the multi-modal fusion. To exploit the sub-feature dependencies we first perform global average pooling to retrieve informative information within each of the d channels of the sub-feature vector. This can be defined by,

$$z_t = F^{GAP}(\eta_t(a, m)) = \frac{1}{A \times M} \sum_{a=1}^A \sum_{m=1}^M \eta_t(a, m), \quad (3)$$

Then a gating mechanism implemented using sigmoid activations is applied to filter out the informative channels within d such that,

$$\beta_t = \sigma(W^2 \times \text{ReLU}(W^1 \times z_t)), \quad (4)$$

The resultant augmented feature vector, β_t , is also of shape $(d, A \times M)$, however, the informative information within is enhanced by considering all the modalities.

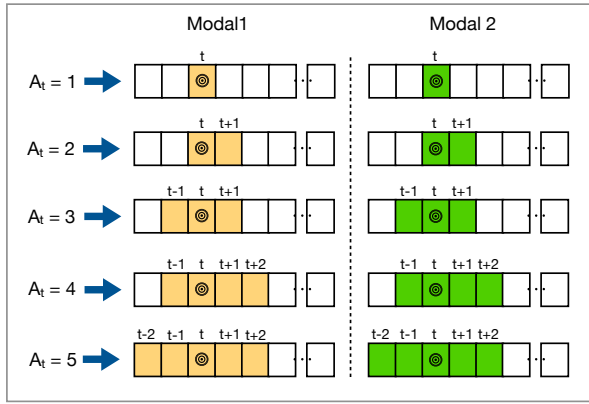


Fig. 3. Illustration of the proposed Attention level parameter, A , and the associated attention scheme. This parameter determines the number of temporal neighbours that a particular frame is associated with, controlling the information flow to the fusion module. For instance if $A = 5$ two neighbouring feature units surrounding the current time step t in each direction (i.e from $t-2$ to t and from t to $t+2$) are selected and processed.

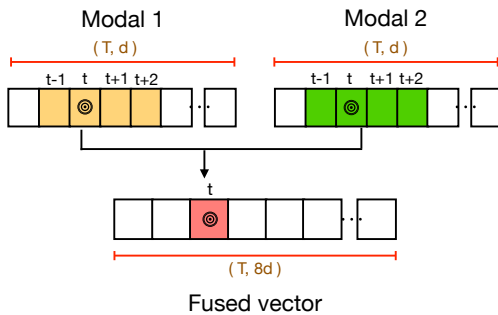


Fig. 4. Illustration of the fusion process when $A = 4$. Features surrounding the current time step t are passed to the proposed fusion block from each modality and it first concatenates them (See. Sec. III-B2). Then it passes the concatenated feature vector through the proposed feature enhancement function which identifies salient feature values in the concatenated vector to enhance, and components to suppress. Utilising this scheme we identify the most informative feature units from the local temporal window for decision making at the current time step.

C. Multi-modal Feature Mapping (MFM) block

The MFM block learns to generate the final gesture classification for the corresponding frame t utilising the fused feature vector β_t . Similar to the UFM, the MFM utilises a series of temporal convolution layers and multiple dilated residual blocks to operate over the fused feature vector, $\beta = [\beta_1, \dots, \beta_T]$. By considering the sequential relationships it generate the frame-wise gesture classifications, $\hat{y}_1, \dots, \hat{y}_T$. This can be written as,

$$\hat{y}_1, \dots, \hat{y}_T = F^{\text{MFM}}([\beta_1, \dots, \beta_T]). \quad (5)$$

D. Loss Formulation

As the classification loss we utilise the cross-entropy loss which is defined as,

$$\mathcal{L}_{ce} = \frac{1}{T} \sum_t -\log(\hat{y}_t). \quad (6)$$

However, only using the frame wise classification loss to learn gesture segmentation is insufficient and can lead to over segmentation errors, even while maintaining high frame wise accuracy. Hence, we also use the smoothing loss is introduced by [10]. This smoothing loss uses the truncated mean squared error over the frame-wise log probabilities. The smoothing loss can be defined as,

$$\mathcal{L}_{sm} = \frac{1}{T \times C} \sum_{t,c} \tilde{\Delta}_{t,c}, \quad (7)$$

where,

$$\tilde{\Delta}_{t,c} = \begin{cases} \Delta_{t,c}, & \text{if } \Delta_{t,c} \leq \tau \\ \tau, & \text{otherwise} \end{cases} \quad (8)$$

and,

$$\Delta_{t,c} = |\log \hat{y}_{t,c} - \log \hat{y}_{t-1,c}|. \quad (9)$$

Here, T , c , $y_{t,c}$ define the number of frames per sequence, number of classes and the probability of class c at time t , respectively. However, during the smoothing loss calculations it only takes the predicted sequence into account without considering it's corresponding ground truth sequence. Furthermore, we observe that it discourages the transition of gestures. Considering this limitation, we propose a novel loss function which we term the mid-point smoothing loss.

Motivated by median filtering in signal denoising we define our mid-point smoothing loss to encourage smooth predictions. However, instead of merely smoothing the predictions, we propose to calculate the distance between the smoothed ground truth and predictions, incorporating a smoothing effect when calculating the loss.

Let w represent a sliding window with N elements. First, we obtain the ground truth gesture class at the mid-point within the window w ,

$$\bar{y} = F^{\text{mid-point}}(y_n), \quad (10)$$

where $n \in w$. Similarly we obtain the predicted gesture class at the mid-point using,

$$\tilde{y} = F^{\text{mid-point}}(\hat{y}_n). \quad (11)$$

Then we define our mid-point smoothing loss,

$$\mathcal{L}_{mid} = \sum_{w \in T} \|\bar{y} - \tilde{y}\|^2. \quad (12)$$

As we are operating over the smoothed ground truth and predicted sequences instead of raw sequences, we observe that this loss component accounts for smooth alignment between ground truth and predictions.

Finally, all three loss functions are summed to form the final loss,

$$\mathcal{L} = \mathcal{L}_{ce} + \lambda_1 \mathcal{L}_{sm} + \lambda_2 \mathcal{L}_{mid}, \quad (13)$$

where, λ_1 and λ_2 are model hyper-parameters that determine the contribution of the different losses.

E. Implementation details

The pre-trained features are extracted by using a ResNet50 network, and features are extracted from the flatten layer. The UFM block is composed of $k = 12$ dilated residual layers, while the MFM block contains $k' = 10$ dilated residual layers. Similar to [10], we double the dilation factor at each layer. We use the Adam optimiser with a learning rate of 0.0005. The implementation of the proposed framework is completed using PyTorch [35].

IV. EXPERIMENTS

A. Datasets

We evaluate our model on two challenging public datasets, EgoGesture [11] and IPN hand [4]. Both datasets are comprised of unsegmented videos containing more than one gestures per video.

EgoGesture dataset [11] is the largest egocentric gesture dataset available for segmented and unsegmented (continuous) gesture classification and is composed of static and dynamic gestures. The dataset contains various challenging scenarios including a static subject with a dynamic background, a walking subject with a dynamic background, cluttered backgrounds, and subjects facing strong sunlight. In our work we utilise the unsegmented continuous gesture data which is more challenging as it requires us segment and recognise the gesture in a single pass. The dataset consists of 84 classes (83 gesture classes and the non-gesture class) recorded in 6 diverse indoor and outdoor settings. The dataset contains 1,239, 411 and 431 videos for training, validation and testing purposes respectively. The dataset provides RGB and depth videos.

IPN hand dataset [4] is a recently released dataset that supports continuous gesture recognition. The dataset contains videos based on 13 static/dynamic gesture classes and a non-gesture class. The gestures are performed by 50 distinct subjects in 28 diverse scenes. The videos are collected under extreme illumination conditions, and static and dynamic backgrounds. The dataset contains a total of 4,218 gesture instances and 800,491 RGB frames. Compared to other publicly available hand gesture datasets, IPN Hand includes the largest number of continuous gestures per video, and has the most rapid transitions between gestures [4]. We utilise the IPN hand dataset specifically as it is provided with multiple modalities:

RGB, optical flow and hand segmentation data; which enables us to demonstrate the scalability (Sec. IV-C4) of the proposed framework.

B. Evaluation Metrics

Mean Jaccard Index (MJJ): To enable state-of-the-art comparisons, we utilise the MJJ to evaluate the model on the EgoGesture dataset as suggested in [11], [36]. For a given input, the Jaccard index measures the average relative overlap between the ground truth and the predicted class label sequence. The Jaccard index for the i^{th} class is calculated using,

$$J_{s,i} = \frac{G_{s,i} \cap P_{s,i}}{G_{s,i} \cup P_{s,i}}, \quad (14)$$

where $G_{s,i}$ and $P_{s,i}$ represents the ground truth and predictions of the i^{th} class label for sequence s respectively. Then the Jaccard index for the sequence can be computed by,

$$J_s = \frac{1}{l_s} \sum_{i=1}^L J_{s,i}, \quad (15)$$

where L is the number of available gesture classes and l_s represents unique true labels. Then, the final mean Jaccard index of all testing sequences is calculated,

$$\bar{J}_s = \frac{1}{n} \sum_{j=1}^n J_{s,j}. \quad (16)$$

Levenshtein Accuracy (LA): In order to evaluate the IPN hand dataset we use the Levenshtein accuracy metric used by [4]. The Levenshtein accuracy is calculated by estimating the Levenshtein distance between the ground truth and the predicted sequences. The Levenshtein distance counts the number of item-level changes between the sequences and transforms one sequence to the other. However, after obtaining the Levenshtein distances, the Levenshtein accuracy is calculated by averaging this distance over the number of true target classes (T_p), and subtracting the average value from 1 (to obtain the closeness) and multiplied by 100 to obtain a percentage,

$$LA = 1 - \frac{l_d}{T_p} \times 100\%. \quad (17)$$

C. Evaluations

1) Selection of Parameter Value, A: In order to decide on the attention level parameter, A , we have evaluated the model on the EgoGesture dataset by increasing the value of A . Figure 5 illustrates the impact of the attention-level parameter on the Jaccard index score for the EgoGesture validation set. Note that $A = 1$ is simple concatenation of the features.

As an attention level of 8 produces the best results, we use $A = 8$ for rest of the evaluations.

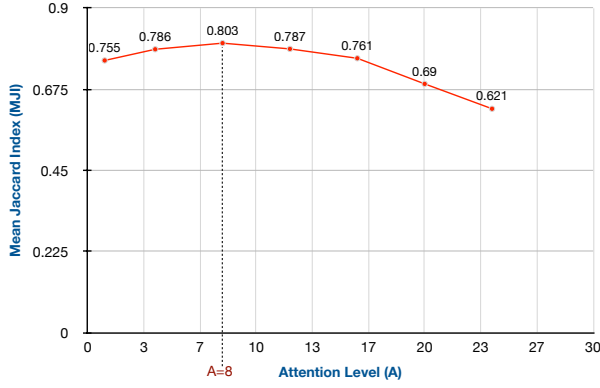


Fig. 5. The change in Jaccard index score with as the attention level parameter, A , is varied.

2) *State-of-the-art Comparison:* In Table I, we compare the performance of the proposed method with the current state-of-the-arts using the EgoGesture dataset. It should be noted that the comparison is done using continuous video streams containing multiple gestures in each videos (not pre-segmented videos containing a single gesture per video). For the evaluations, the Jaccard index (as described in IV-B) is used. Similar to the original work [11], we use two settings in evaluating the results. In both settings we keep the sliding window (sw) length at 16 while we consider strides of 16 ($l=16, s=16$) and 8 ($l=16, s=8$). In [11], the authors obtain the label predictions by considering the class probabilities of each clip predicted by the C3D softmax layer. Here, the sliding window is applied over the whole sequence to generate a video clip. For the setting where the sliding window overlaps (i.e. $l=16, s=8$), frame label predictions are obtained by accumulating the classification scores of two overlapped windows and the most likely class is chosen as the predicted label for each frame.

Other than utilising the C3D model, the authors in [11] have further improved the gesture prediction method by employing a Spatio-Temporal Transfer Module (STTM) [29] (denoted sw+C3D+STTM) and an LSTM network (denoted LSTM+C3D). In LSTM+C3D, the class labels of each frame are predicted by an LSTM based on the C3D features extracted at the current time slice. An LSTM with hidden feature dimension of 256 is used. The authors have gained better results by employing the LSTM network. However, in both settings, our proposed multi-modal fusion method is able to outperform the current state-of-the-art methods for the EgoGesture dataset by a considerable margin. We also obtained 1.9% gain (metric calculation of MJ (see Sec. IV-B)) using the second setting (i.e. $l=16, s=8$) where the the sliding windows overlap.

We also evaluate our proposed model on the IPN Hand dataset [4] and Table II includes a comparison of our proposed fusion model with the state-of-the-art. The results use the Levenshtein accuracy metric (see IV-B). In the original work [4], the authors have performed continuous gesture recognition by using a two-stage approach where at the first stage a separate detection model is used to detect gestures within a sequence. For this task binary classification is carried out to

TABLE I
COMPARISON OF OUR PROPOSED METHOD WITH THE STATE-OF-THE-ART METHODS ON THE EGOGESTURE DATASET. RESULTS ARE SHOWN USING THE MJ METRIC (SEE SEC. IV-B).

Method	MJ
sw+C3D ($l=16, s=16$) [11]	0.618
sw+C3D ($l=16, s=8$) [11]	0.698
sw+C3D+STTM ($l=16, s=8$) [11]	0.709
LSTM+C3D ($l=16, s=8$) [11]	0.718
Proposed ($l=16, s=16$)	0.784
Proposed ($l=16, s=8$)	0.803

separate gestures from non-gestures using a ResLight-10 [6] model. In the second stage the detected gesture is classified by the classification model (ResNet50 or ResNetXt-101). For the overall process in [4], the authors have considered different combinations of data modalities such as RGB-Flow and RGB-Seg where 'Flow' and 'Seg' refer to optical flow and semantic segmentation respectively. However, the authors gained the highest classification results for the ResNetXt-101 with RGB-Flow data.

In contrast to the two-stage approach introduced in [4], we use a single-stage method which directly predicts the sequence of gesture class labels for the entire frame sequence of the video. Even though such a direct approach is challenging and requires a high level of discriminating ability within the model to separate multiple gesture and non-gesture classes, our fusion model outperforms the state-of-the-art results on IPN hand dataset by a significant margin. In Sec. IV-C4 we further evaluate the model using the three available modalities of RGB, flow and semantic segmentation outputs, illustrating the scalability of the proposed framework.

TABLE II
COMPARISON OF OUR PROPOSED METHOD WITH THE STATE-OF-THE-ART METHOD ON THE IPN HAND DATASET. THE RESULTS ARE SHOWN IN TERM OF LEVENSHTIN ACCURACY (SEE SEC. IV-B).

Method	Modality	Results
ResNet50 [4]	RGB-Seg	33.27
ResNet50 [4]	RGB-Flow	39.47
ResNetXt-101 [4]	RGB-Seg	39.01
ResNetXt-101 [4]	RGB-Flow	41.47
Proposed	RGB-Flow	68.12

In addition to the quantitative results, we provide qualitative results (in Fig. 6 and Fig. 7) where we visualise the temporal gesture predictions generated by the proposed method for different frame sequences from EgoGesture and IPN Hand datasets respectively.

As shown in Fig. 6, even with the higher number of gesture classes (84 classes including the non-gesture class) in the EgoGesture dataset, the model is able to detect the gestures well. We noticed in only a few cases the gesture 'snap_fingers' (in Fig. 6(b), bottom) is poorly detected and the model seems to struggle to locate the actual gesture class. Apart from a small number of instances where the model faces difficulties to predict the gesture class, the model learned the non-gesture to gesture transitions well. Similarly in Fig. 7 and the predictions obtained for the IPN Hand dataset, the model

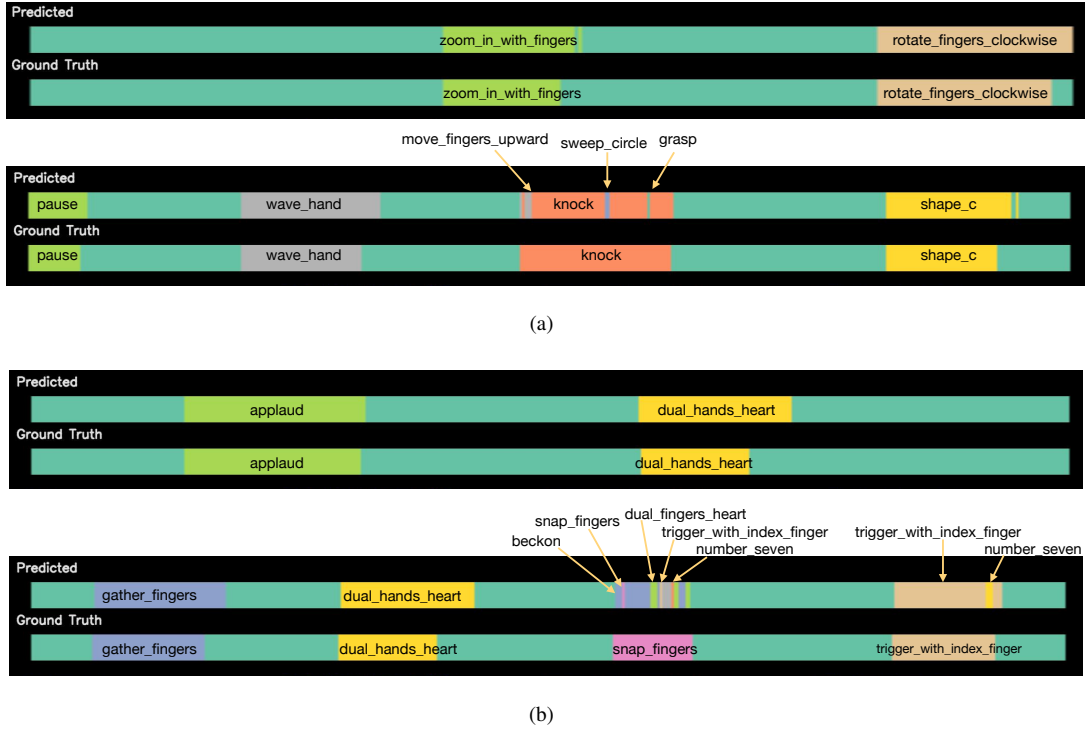


Fig. 6. Qualitative results of the propose model predictions on EgoGesture dataset.

shows good performance even in the presence of the rapid action changes in the dataset. According to the publishers of the dataset, the IPN hand dataset contains the largest number of continuous gestures per video, which is understandable when comparing the timelines shown in Fig. 6 and Fig. 7.

3) *Impact of Loss Formulation*: We investigate the impact of our proposed loss formulation, which enhances the overall learning of the introduced model. In Table III, the MJI of the EgoGesture dataset obtained with different loss formulations is shown. In the table, \mathcal{L}_{ce} , \mathcal{L}_{sm} and \mathcal{L}_{med} represents the cross-entropy loss (Eq. 6), the smoothing loss (Eq. 7) and mid-point smoothing loss (Eq. 12) respectively. Note that the combination of all three losses is the loss used by the proposed approach, $\mathcal{L}_{overall}$ (Eq. 13).

TABLE III

THE IMPACT OF DIFFERENT LOSS FORMULATIONS: WE COMPARE THE MJI ON THE EGOGESTURE DATASET WITH DIFFERENT LOSS FORMULATIONS. HERE, \mathcal{L}_{ce} , \mathcal{L}_{sm} AND \mathcal{L}_{med} REPRESENT THE CROSS-ENTROPY LOSS (EQ. 6), THE SMOOTHING LOSS (EQ. 7) AND MID-POINT SMOOTHING LOSS (EQ. 12) RESPECTIVELY.

Loss	MJI
\mathcal{L}_{ce}	0.753
$\mathcal{L}_{ce} + \mathcal{L}_{sm}$	0.781
$\mathcal{L}_{ce} + \mathcal{L}_{mid}$	0.784
$\mathcal{L}_{ce} + \mathcal{L}_{mid} + \mathcal{L}_{sm}$	0.803

From Table III we observe that both losses, \mathcal{L}_{mid} and \mathcal{L}_{sm} have contributed to improving the the cross-entropy loss, with the proposed mid-point based smoothing mechanism showing a slightly higher improvement. However, we observe a significant improvement when utilising all the losses together,

illustrating the importance of mid-point based comparison of different predicted and ground-truth windows.

4) *Scalability of the Fusion Block*: In order to illustrate the scalability of the proposed framework and fusion mechanism to different numbers of modalities, we make use of a third modality: the segmentation maps which are provided in the IPN Hand dataset.

To make the feature extraction of hand segmentation maps more meaningful, we use the Pix-to-Pix GAN introduced in [32]¹. We first train the GAN to generate hand segmentation maps that are similar to the ones provided with the IPN hand dataset. We set the number of filters in generator and the discriminator to 8 and train the GAN by following the original work. After GAN training, we use the trained generator model for feature extraction of the third modality where features are obtained from the bottleneck layer of the generator. These extracted feature vectors (of dimension $18 \times 18 \times 8 = 2592$) are fed to the third UFM model along side the UFM models used for the RGB and optical flow based feature vectors, as per the model evaluated in Tab. II. It should be noted that having varying feature vector dimensions (i.e 2592 for segmentation map inputs while 2048 for RGB and optical flow features) does not effect the fusion as the UFM block maps the feature vectors to the same dimensionality at the output head which is the input to the fusion block. As expected, with the use of three modalities we were able to improve the overall Levenshtein accuracy by 1.8% from the setting with only 2 modalities, achieving a Levenshtein accuracy of 69.92% with the 3 feature modalities. With this evaluation

¹We use the implementation provided at <https://github.com/junyanz/pytorch-CycleGAN-and-pix2pix>

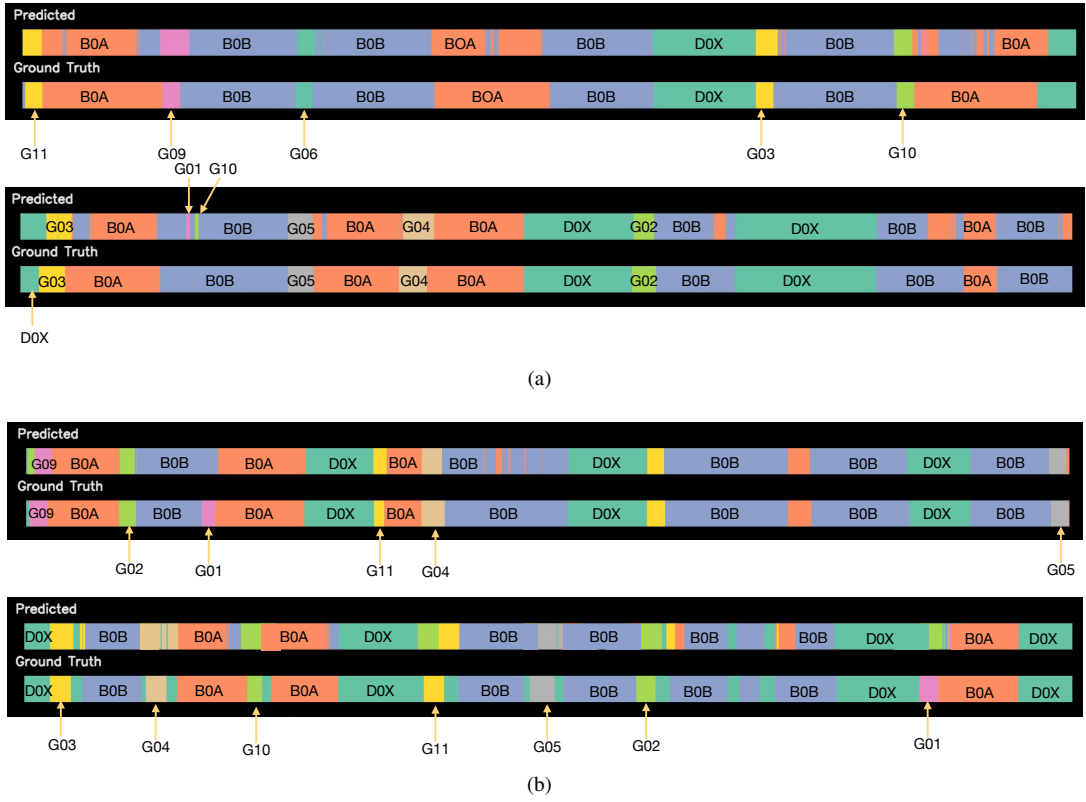


Fig. 7. Qualitative results of the propose model predictions on IPN Hand dataset.

we illustrate that the proposed method can seamlessly be extended to fuse the data from a different number of modalities with different feature dimensions. Despite the challenge this brings, our method has been able to successfully extract salient features to support the decision making process.

5) *Ablation Experiment*: In order to demonstrate the importance of the proposed fusion mechanism we conducted an ablation experiment. In the experiment, we gradually remove components of the proposed framework and re-train and test the models with the EgoGesture dataset. In Table IV, we report the evaluation results for five ablation models with the MJJ metric. The ablation models are formulated as follows.

- **Only RGB**: A single UFM block is utilised for the RGB stream and the output of the uni-modal block is passed directly through the MFM block (see Fig. 8 (a)). Here, the MFM block works as a second uni-modal network as only a single modality is used. Therefore, the proposed feature enhancer (FE) is not used.
- **Only Depth**: The model is similar to that of the 'Only RGB' stream ablation model ((see Fig. 8 (a))). However, the instead of the input RGB stream, the depth input stream is used.
- **Simple Fusion**: Our proposed framework is utilised without the introduced fusion block. The fusion is performed by performing concatenation along the sequence of RGB and depth modalities. The model architecture is further illustrated in Fig 8 (b).
- **Proposed w/o FE**: The proposed framework without the feature enhancer (FE) module is utilised.

TABLE IV
EVALUATION RESULTS FOR THE ABLATION MODELS USING THE EGOGESTURE DATASET.

Model	MJJ
Only RGB	0.697
Only Depth	0.741
Simple Fusion	0.755
Proposed w/o FE	0.792
Proposed	0.803

A key observation based on the results presented in IV is that naive concatenation of multi-modal features does not generate helpful information for continuous gesture recognition. We observe a performance drop of approximately 5% when simple concatenation is applied in comparison to the proposed approach, and only slight improvement for naive concatenation over the best individual model (depth). The proposed temporal fusion strategy as well as the feature enhancement block have clearly contributed to the superior results that we achieve.

V. CONCLUSION

We propose a single-stage continuous gesture recognition method with a novel fusion method to perform multi-modal feature fusion. The proposed framework can be applied to varying length gesture videos, and able is to perform the gesture detection and classification directly in a single step without the help of an additional detector model. The proposed fusion model is introduced to handle multiple modalities without a restriction on the number of modes, and further

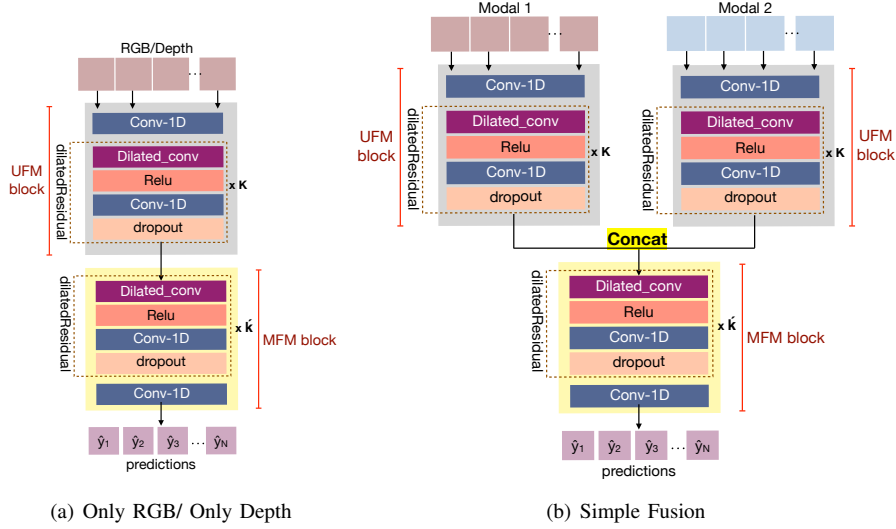


Fig. 8. Ablation models: (a) The models that utilise a single modality (Only RGB/ Only Depth) are composed of a single UFM and MFM blocks where the MFM block works as a second uni-modal network. (b) The Simple Fusion model is formulated by performing concatenation along the sequence of RGB and depth modalities instead of utilising the proposed fusion block.

experiments demonstrate the scalability of the fusion method and show how the multiple streams complement the overall gesture recognition process. With the proposed loss formulation our introduced single-stage continuous gesture recognition framework learns the gesture transitions with considerable accuracy, even with the rapid gesture transitions of the IPN hand dataset. The ablation experiment further highlights the importance of the components of the proposed method, which outperformed the state-of-the-art systems on both datasets by a significant margin. Our model has applications to multiple real-world domains that require classification on continuous data, while the fusion model is applicable to other fusion problems where videos or signal inputs are present, and can be used with or without the UFM or MFM blocks.

ACKNOWLEDGMENT

The research presented in this paper was supported by an Australian Research Council (ARC) Discovery grant DP170100632.

REFERENCES

- [1] H. R. V. Joze, A. Shaban, M. L. Iuzzolino, and K. Koishida, "Mmtm: Multimodal transfer module for cnn fusion," in *Proceedings of the IEEE/CVF Conference on Computer Vision and Pattern Recognition*, 2020, pp. 13 289–13 299.
- [2] P. Molchanov, S. Gupta, K. Kim, and J. Kautz, "Hand gesture recognition with 3d convolutional neural networks," in *Proceedings of the IEEE conference on computer vision and pattern recognition workshops*, 2015, pp. 1–7.
- [3] P. Molchanov, S. Gupta, K. Kim, and K. Pulli, "Multi-sensor system for driver's hand-gesture recognition," in *2015 11th IEEE international conference and workshops on automatic face and gesture recognition (FG)*, vol. 1, 2015, pp. 1–8.
- [4] G. Benitez-Garcia, J. Olivares-Mercado, G. Sanchez-Perez, and K. Yanai, "Ipn hand: A video dataset and benchmark for real-time continuous hand gesture recognition," *arXiv preprint arXiv:2005.02134*, 2020.
- [5] N. N. Hoang, G.-S. Lee, S.-H. Kim, and H.-J. Yang, "Continuous hand gesture spotting and classification using 3d finger joints information," in *2019 IEEE International Conference on Image Processing (ICIP)*, 2019, pp. 539–543.
- [6] O. Köpüklü, A. Gunduz, N. Kose, and G. Rigoll, "Real-time hand gesture detection and classification using convolutional neural networks," in *2019 14th IEEE International Conference on Automatic Face & Gesture Recognition (FG 2019)*, 2019, pp. 1–8.
- [7] G. Zhu, L. Zhang, P. Shen, J. Song, S. A. A. Shah, and M. Bennamoun, "Continuous gesture segmentation and recognition using 3dcnn and convolutional lstm," *IEEE Transactions on Multimedia*, vol. 21, no. 4, pp. 1011–1021, 2018.
- [8] P. Gupta, K. Kautz *et al.*, "Online detection and classification of dynamic hand gestures with recurrent 3d convolutional neural networks," in *CVPR*, vol. 1, no. 2, 2016, p. 3.
- [9] C. Lea, M. D. Flynn, R. Vidal, A. Reiter, and G. D. Hager, "Temporal convolutional networks for action segmentation and detection," in *proceedings of the IEEE Conference on Computer Vision and Pattern Recognition*, 2017, pp. 156–165.
- [10] Y. A. Farha and J. Gall, "Ms-tcn: Multi-stage temporal convolutional network for action segmentation," in *Proceedings of the IEEE Conference on Computer Vision and Pattern Recognition*, 2019, pp. 3575–3584.
- [11] Y. Zhang, C. Cao, J. Cheng, and H. Lu, "Egogesture: a new dataset and benchmark for egocentric hand gesture recognition," *IEEE Transactions on Multimedia*, vol. 20, no. 5, pp. 1038–1050, 2018.
- [12] J. Wan, G. Guo, and S. Z. Li, "Explore efficient local features from rgb-d data for one-shot learning gesture recognition," *IEEE transactions on pattern analysis and machine intelligence*, vol. 38, no. 8, pp. 1626–1639, 2015.
- [13] X. Shen, G. Hua, L. Williams, and Y. Wu, "Dynamic hand gesture recognition: An exemplar-based approach from motion divergence fields," *Image and Vision Computing*, vol. 30, no. 3, pp. 227–235, 2012.
- [14] H. Trinh, Q. Fan, P. Gabbur, and S. Pankanti, "Hand tracking by binary quadratic programming and its application to retail activity recognition," in *2012 IEEE Conference on Computer Vision and Pattern Recognition*, 2012, pp. 1902–1909.
- [15] X. Yang and Y. Tian, "Super normal vector for activity recognition using depth sequences," in *Proceedings of the IEEE conference on computer vision and pattern recognition*, 2014, pp. 804–811.
- [16] J. Wang, Z. Liu, J. Chorowski, Z. Chen, and Y. Wu, "Robust 3d action recognition with random occupancy patterns," in *European conference on computer vision*, 2012, pp. 872–885.
- [17] H. Wang and C. Schmid, "Action recognition with improved trajectories," in *Proceedings of the IEEE international conference on computer vision*, 2013, pp. 3551–3558.
- [18] K. Simonyan and A. Zisserman, "Two-stream convolutional networks for action recognition in videos," in *Advances in neural information processing systems*, 2014, pp. 568–576.
- [19] H. Gammulle, S. Denman, S. Sridharan, and C. Fookes, "Predicting the future: A jointly learnt model for action anticipation," in *Proceedings*

- of the *IEEE International Conference on Computer Vision*, 2019, pp. 5562–5571.
- [20] Z. Teng, J. Xing, Q. Wang, B. Zhang, and J. Fan, “Deep spatial and temporal network for robust visual object tracking,” *IEEE Transactions on Image Processing*, vol. 29, pp. 1762–1775, 2019.
 - [21] Z. Shou, D. Wang, and S.-F. Chang, “Temporal action localization in untrimmed videos via multi-stage cnns,” in *Proceedings of the IEEE Conference on Computer Vision and Pattern Recognition*, 2016, pp. 1049–1058.
 - [22] S. Ji, W. Xu, M. Yang, and K. Yu, “3d convolutional neural networks for human action recognition,” *IEEE transactions on pattern analysis and machine intelligence*, vol. 35, no. 1, pp. 221–231, 2012.
 - [23] P. Zhang, J. Xue, C. Lan, W. Zeng, Z. Gao, and N. Zheng, “Eleatt-rnn: Adding attentiveness to neurons in recurrent neural networks,” *IEEE Transactions on Image Processing*, vol. 29, pp. 1061–1073, 2019.
 - [24] Z. Liu, X. Chai, Z. Liu, and X. Chen, “Continuous gesture recognition with hand-oriented spatiotemporal feature,” in *Proceedings of the IEEE International Conference on Computer Vision Workshops*, 2017, pp. 3056–3064.
 - [25] L. Li, S. Qin, Z. Lu, K. Xu, and Z. Hu, “One-shot learning gesture recognition based on joint training of 3d resnet and memory module,” *Multimedia Tools and Applications*, vol. 79, no. 9, pp. 6727–6757, 2020.
 - [26] Y. Zhang, L. Shi, Y. Wu, K. Cheng, J. Cheng, and H. Lu, “Gesture recognition based on deep deformable 3d convolutional neural networks,” *Pattern Recognition*, vol. 107, p. 107416, 2020.
 - [27] B. Su, J. Zhou, X. Ding, and Y. Wu, “Unsupervised hierarchical dynamic parsing and encoding for action recognition,” *IEEE Transactions on Image Processing*, vol. 26, no. 12, pp. 5784–5799, 2017.
 - [28] M. Abavisani, H. R. V. Joze, and V. M. Patel, “Improving the performance of unimodal dynamic hand-gesture recognition with multimodal training,” in *Proceedings of the IEEE Conference on Computer Vision and Pattern Recognition*, 2019, pp. 1165–1174.
 - [29] C. Cao, Y. Zhang, Y. Wu, H. Lu, and J. Cheng, “Egocentric gesture recognition using recurrent 3d convolutional neural networks with spatiotemporal transformer modules,” in *Proceedings of the IEEE International Conference on Computer Vision*, 2017, pp. 3763–3771.
 - [30] H. Gammulle, T. Fernando, S. Denman, S. Sridharan, and C. Fookes, “Coupled generative adversarial network for continuous fine-grained action segmentation,” in *2019 IEEE Winter Conference on Applications of Computer Vision (WACV)*, 2019, pp. 200–209.
 - [31] H. Gammulle, S. Denman, S. Sridharan, and C. Fookes, “Fine-grained action segmentation using the semi-supervised action gan,” *Pattern Recognition*, vol. 98, p. 107039, 2020.
 - [32] P. Isola, J.-Y. Zhu, T. Zhou, and A. A. Efros, “Image-to-image translation with conditional adversarial networks,” in *Proceedings of the IEEE conference on computer vision and pattern recognition*, 2017, pp. 1125–1134.
 - [33] A. v. d. Oord, S. Dieleman, H. Zen, K. Simonyan, O. Vinyals, A. Graves, N. Kalchbrenner, A. Senior, and K. Kavukcuoglu, “Wavenet: A generative model for raw audio,” *ISCA Speech Synthesis Workshop (SSW)*, 2016.
 - [34] J. Hu, L. Shen, S. Albanie, G. Sun, and E. Wu, “Squeeze-and-excitation networks,” *IEEE transactions on pattern analysis and machine intelligence*, 2019.
 - [35] A. Paszke, S. Gross, F. Massa, A. Lerer, J. Bradbury, G. Chanan, T. Killeen, Z. Lin, N. Gimelshein, L. Antiga *et al.*, “Pytorch: An imperative style, high-performance deep learning library,” in *Advances in neural information processing systems*, 2019, pp. 8026–8037.
 - [36] J. Wan, Y. Zhao, S. Zhou, I. Guyon, S. Escalera, and S. Z. Li, “Chalearn looking at people rgb-d isolated and continuous datasets for gesture recognition,” in *Proceedings of the IEEE Conference on Computer Vision and Pattern Recognition Workshops*, 2016, pp. 56–64.